Princeton Plasma Physics Laboratory

PPPL-4030

PPPL-4030

Experimental Studies of Anode Sheath Phenomena in a Hall Thruster Discharge

L. Dorf, Y. Raitses, and N.J. Fisch

December 2004

PPPL
PRINCETON PLASMA PHYSICS LABORATORY

Prepared for the U.S. Department of Energy under Contract DE-AC02-76CH03073.

PPPL Report Disclaimers

Full Legal Disclaimer

Trademark Disclaimer

PPPL Report Availability

This report is posted on the U.S. Department of Energy's Princeton Plasma Physics Laboratory Publications and Reports web site in Fiscal Year 2005. The home page for PPPL Reports and Publications is: http://www.pppl.gov/pub_report/

Office of Scientific and Technical Information (OSTI):

Available electronically at: http://www.osti.gov/bridge.

Available for a processing fee to U.S. Department of Energy and its contractors, in paper from:

U.S. Department of Energy
Office of Scientific and Technical Information
P.O. Box 62
Oak Ridge, TN 37831-0062

Telephone: (865) 576-8401

Fax: (865) 576-5728

E-mail: reports@adonis.osti.gov

National Technical Information Service (NTIS):

This report is available for sale to the general public from:

U.S. Department of Commerce
National Technical Information Service
5285 Port Royal Road
Springfield, VA 22161

Telephone: (800) 553-6847

Fax: (703) 605-6900

Email: orders@ntis.fedworld.gov

Online ordering: http://www.ntis.gov/ordering.htm

Experimental Studies of Anode Sheath Phenomena in a Hall Thruster Discharge

L. Dorf*, Y. Raitses and N. J. Fisch

Princeton Plasma Physics Laboratory (PPPL), Princeton, NJ 08543

(Received

Both electron-repelling and electron-attracting anode sheaths in a Hall thruster were characterized by measuring the plasma potential with biased and emissive probes [L. Dorf, Y. Raitses, V. Semenov and N.J. Fisch, Appl. Phys. Let. **84**, 1070 (2004)]. In the present work, two-dimensional structures of the plasma potential, electron temperature, and plasma density in the near-anode region of a Hall thruster with clean and dielectrically coated anodes are identified. Possible mechanisms of anode sheath formation in a Hall thruster are analyzed. The path for current closure to the anode appears to be the determining factor in the anode sheath formation process. The main conclusion of this work is that the anode sheath formation in Hall thrusters differs essentially from that in the other gas discharge devices, like a glow discharge or a hollow anode, because the Hall thruster utilizes long electron residence times to ionize rather than high neutral pressures.

* Present address: Los Alamos National Laboratory, Los Alamos, NM 87544

I. INTRODUCTION

In a gas discharge, there can be either an increase or a drop in the plasma potential over a distance of a few Debye lengths from the anode, generally referred to in the literature as the "anode fall" (Fig. 1). When the anode is at a higher potential than the near-anode plasma, the anode fall is called "positive", and when it is at a lower potential – "negative". The positive and negative anode falls are associated with formation of the electron-attracting and electron-repelling anode sheaths, respectively. The anode sheath is a thin space-charge layer adjoint to the electrode. It is a non-linear structure that was first observed and studied by Langmuir and Mott-Smith in glow discharges.[1]

Anode sheath phenomena were studied comprehensively in other discharge devices such as a glow discharge,[2] which, as a Hall thruster (HT), is characterized by the discharge currents of no more than a few amperes, and a hollow anode plasma source,[3-5] which, as a Hall thruster, is characterized by a relatively high degree of ionization, compared to that of the glow discharge. However, both glow discharge and hollow anode plasma source typically operate at much higher neutral gas pressures (tens to hundreds of militorrs vs. few militorrs in a HT); a hollow anode plasma source is also characterized by much smaller discharge currents (tens of miliamperes vs. amperes in a HT).

Experimental studies of the anode fall in glow discharges showed that at typical operating conditions the anode fall at a plane anode is positive.[2,6-9] At these conditions, the ion current flowing into a positive column is generated by ionization in a thin space-charge layer near the anode, with a voltage drop of the order of ionization potential of the working gas.[8-10] At higher discharge currents, of the order of several to ten amperes, the anode fall in the same discharge was observed to be negative[2] (note that at such high

currents, a “glow discharge” is no longer an appropriate name for a low pressure gas discharge). In this case, the thermal electron current to the anode, produced by ionization in the quasineutral plasma, is larger than the discharge current. Therefore, the formation of a negative fall is required to repel the excessive electron flux from the anode.[1,8] It is was also observed experimentally for glow discharges that a decrease of the anode collecting surface area leads to altering of the anode fall from negative to positive.[2]

Furthermore, under certain conditions described later in this work, the near-anode region of a Hall thruster discharge can be compared to that of a hollow-anode plasma source.[3,4] A high degree of ionization inside the hollow-anode plasma source was attributed to formation of a thick electron-attracting anode sheath, in which electrons gain kinetic energy of up to 40 eV.[5] Thus, the formation of a positive fall in a Hall thruster might be explained by the need for enhanced ionization; i. e. additional ionization in the sheath or inside the anode, which would increase the electron flux toward the anode collecting surface to the value determined by the discharge current. This and other possible mechanisms of anode fall formation require detailed investigation.

In spite of a number of experimental[11-22] and theoretical[23-26] studies of a Hall thruster internal plasma structure, the understanding of the anode sheath phenomena in Hall thrusters was, until recently, very limited. A more detailed review of previous works and additional motivation for studying the anode sheath phenomena in Hall thrusters can be found in Refs. 27 and 28. As was reported recently, a diagnostic apparatus comprising biased and emissive electrostatic probes, a high-precision positioning system, and low-noise electronic circuitry was developed and used for measurements in the near-anode region of the 12.3 cm Hall thruster operating in the 0.2 – 2 kW power range[27,29].

Accurate, non-disturbing measurements of the plasma potential allowed the first experimental identification of both electron-repelling (negative anode fall) and electron-attracting (positive anode fall) anode sheaths in a HT. Most interestingly, an intricate new phenomenon revealed by the probe measurements is that the anode fall changes from positive to negative upon removal of the dielectric coating, which appears on the anode surface during the course of HT operation. The dependence of the sign and magnitude of the anode sheath on the discharge voltage and mass flow rate was also studied in Ref. 27, and the results of this investigation were found to be in agreement with our recent theoretical model.[27,28,30] Particularly, it was found that when the electron temperature, T_e, in the channel increases with the discharge voltage, V_d, the magnitude of the negative anode fall at a clean anode also increases with V_d.

In this paper, we again use the dielectric coating which appears on the anode surface as a natural way of decreasing the anode collecting surface area, and continue to study the anode sheath phenomena in the 2 kW Hall thruster for two different operating regimes – with clean and with coated anodes. A significant number of the biased probe measurements results only partially reported in Ref. 27 are presented in this work; the nature of the dielectric coating is identified; and, most importantly, possible mechanisms of anode sheath formation in a Hall thruster are analyzed.

The article is divided into five sections. In Sec. II, we report our most recent findings about the nature of the anode dielectric coating, and present pictures of the clean and coated anodes. In Sec. III, two-dimensional structures of the plasma potential, electron temperature, and plasma density in the near-anode region of a Hall thruster with clean and coated anodes are identified; also, the visual evidence of 2 kW Hall thruster

operation in both cases is presented. In Sec. IV, possible mechanisms of anode sheath formation in a Hall thruster with clean and coated anodes are analyzed. We conclude in Sec. V with discussing possible practical implications of this work.

II. ANODE DIELECTRIC COATING

It was observed experimentally for the 2 kW Hall thruster in this study that a dielectric coating appears on the anode surface exposed to plasma after the thruster accumulates about 10 or more hours of lifetime, operating at typical conditions (Fig. 2). A layer of coating was typically thin – about several tens of microns – and ranged in color from blue-green to golden-brown, with sometimes several colors present on the same coated anode. In some cases, after several tens of hours of thruster operation, the coating would accumulate to be up to 0.1 mm thick, and then it would split off – the scraps of coating were found at the bottom part of the channel. Furthermore, distinctive spots were observed next to each of the gas-injecting holes hidden under the gas-mixing baffles (Fig. 2).

To identify the chemical composition of the coating, three small samples were inserted under the baffle at the bottom part of the anode. Two samples were made out of the same material as the anode – stainless steel – and one sample was made out of tantalum. After several hours of thruster operation, the samples were extracted and a dielectric coating was observed on each of the samples. The coating on the tantalum sample was of a homogeneous blue-green color, and the coating on the stainless steel samples was of a yellow-red color. The coatings on all three samples were then analyzed using energy dispersion spectroscopy (EDS). Results of EDS analysis – *counts per energy* spectra of the X-ray radiation emitted by the atoms of the coating as a result of

electron bombardment – are reported in Ref. 28. It was ultimately decided that the coatings on all three samples are essentially the oxides of the substrate materials. The anode material, stainless steel, can indeed be expected to get oxidized during thruster operation, since the anode temperature could reach about 1000 C at typical thruster operating conditions.

It is still unclear, however, how oxygen gets into the thruster channel. Impurity limits data[28] for a research grade Xenon used in the presented experiments suggests that only insignificant amount of oxygen enters the channel along with the xenon propellant, since the percentage of O_2 in the cylinder containing the supply of xenon is very low – less than 0.1 ppm (parts per million). It can alternatively be suggested that the presence of oxygen in the thruster channel is the vacuum facility effect – ougassing of the vacuum vessel walls, cryogenic pumps interior, and stainless steel gas feed tubes could be one of the sources of oxygen, for example (note that the gas system was leak tested using Inficon UL200 helium leak detector, and the leak rate was observed to be in the range of $10^{-8}\,\mathrm{mbar}\cdot\mathrm{l/s} \approx 6\cdot10^{-7}\,\mathrm{SCCM}$). A detailed investigation of oxygen origination and its content in the vacuum vessel needs to be conducted with the use of a residual gas analyzer (RGA) that is already installed on one of the ports of the Hall Thruster Experiment (HTX) vacuum vessel. Information about the content of oxygen in the background gas inside the vacuum vessel can then be used to estimate the anode surface oxidation rate and coating formation time.

III. NEAR-ANODE PLASMA STRUCTURE MEASUREMENTS

To investigate the effect of the anode collecting surface area on the anode sheath, the electrostatic probe apparatus described in Ref. 29 was employed for measurements in the

near-anode region of the 2 kW Hall thruster with clean and coated anodes.[27] The thruster has a conventional annular configuration with a channel length of 4.6 cm (which is in the 2 – 8 cm range typical for HTs [11-22]) and a channel width of 2.5 cm [Fig. 4 (a)]. Typically, the thruster was operated at xenon gas mass flow rates of $\dot{m} = 2 - 5$ mg/s, and in the discharge voltage range of $V_d = 200 - 450$ V. In these experiments, the magnetic field was kept constant (B ~ 100 Gauss near the exit, at the mid-point between the channel walls). Figure 4 (b) shows results of non-linear simulations of the magnetic field distribution. Simulations were conducted using measured B-H curve of the low carbon steel used in the thruster design. A comparison of simulated and measured results showed a very good agreement.

The plasma potential, plasma density and electron temperature were measured at 2, 7 and 12 mm from the anode with the biased electrostatic probe. The probe was introduced radially into the near-anode region through the axial slot made in the outer channel wall. The plasma measurements were performed at several distances from the thruster axis: at the outer wall (OW), R = 62 mm, in the mid-point between the channel walls (MC), R = 49 mm, and at 4 mm from the inner wall (IW), R = 41 mm. After the first set of experiments, the dielectric coating, which appears on the anode surface in the course of thruster operation, was removed, and a second set of experiments was conducted.

Figures 4 (a) – 6 (a) and 4 (b) – 6 (b) show the results of biased probe measurements in the near-anode region of the 2 kW Hall thruster with the clean and coated anodes, respectively, for $\dot{m} = 5$ mg/s. Zero potential is chosen at the anode. The error bars shown in the plasma potential plots were computed using the error analysis described in Ref. 29. As can be seen from Fig. 4 (a), in the case of the clean anode, the plasma potential at 2 –

12 mm from the anode is higher than the anode potential – the anode fall is negative. This indicates the presence of an electron-repelling anode sheath predicted theoretically in Hall.[23] Although there are many experimental studies of the HT plasma structure[11,14-22], this appears to be the first experimental observation of the electron-repelling anode sheath in Hall thrusters.

As can be seen from Fig. 4 (b), in the case of the coated anode, the plasma potential at 2 – 12 mm from the anode is lower than the anode potential – the anode fall is positive. This indicates the presence of an electron-attracting anode sheath. Furthermore, it was observed that thruster operation with a coated anode is associated with a visual effect: the gas-injecting holes glow brighter than the rest of the anode, with appearance of a jet-like structure from each hole [Fig. 7 (b)]. When the anode front surface is coated with dielectric, the discharge current supposedly closes to the anode at the surfaces hidden under the baffles (Fig. 2), as these surfaces can remain conductive. Despite the fact that the plasma density measured near the coated anode is almost twice as large as that for the clean anode (Fig. 6), total thermal current carried by the electrons entering the volume under the baffles is significantly smaller than the discharge current. An additional electron flux supposedly gets drawn in under the baffles by the electron-attracting sheath that appears near the inner, metal sides of the baffles. In the next section, the above phenomena are discussed in greater detail.

Another interesting observation that can be readily made from Fig. 4 is that the plasma potential has a tendency to increase toward the outer channel wall for both clean and coated anodes. However, the electron (plasma) density has a tendency to decrease toward the outer wall in the case of the coated anode, and in the case of the clean anode,

the radial structure of the electron density depends on the discharge voltage (Fig. 6). Assuming Boltzman distribution for electrons in the near-anode plasma, where magnetic field and collision frequency are very small, one should expect the electron density to be higher where the plasma potential is higher. This discrepancy between the measured and expected behavior of the plasma potential and electron density is not yet understood. It could be associated, for example, with a non-Maxwellian shape of the electron distribution function, which was observed in Hall thrusters.[31]

IV. POSSIBLE MECHANISMS OF ANODE FALL FORMATION

A. Neutral Density Distribution

To understand anode sheath formation, first it is useful to analyze the distribution of the neutral density near and inside the anode. For $\dot{m} = 5\,\text{mg/s}$, rough density estimations yield that mean free path for neutral-neutral collisions inside the anode and gas-injecting holes, $\Lambda_H \sim 0.1\,\text{mm}$, is smaller than the diameter of the hole, D_H = 0.3 mm (Fig. 8), so hydrodynamic Bernoulli equation for neutral pressure, P_n, neutral density, n_n, and neutral flow velocity, V_n, can be employed to relate flows inside the holes and inside the anode: $P_n + M_n n_n V_n^2/2 = Const$, where $M_n = 2.2 \cdot 10^{-22}\,\text{g}$ is the mass of a Xenon atom.[32] Taking into account the flow continuity equation along with the fact that the cross-sectional area of the anode cavity (almost equal to the collecting surface area of the clean anode, $A_{coll} = 77\,\text{cm}^2$) is much larger than the combined cross-sectional area of the holes, $A_H = 0.03\,\text{cm}^2$, the dynamic pressure term can be neglected inside the anode. Similar to the problem of the flow of gas through the nozzle,[32] the neutral flow is assumed to have a sonic velocity inside the holes. For the isothermal flow with the

neutral temperature equal to the anode temperature, $T_A \approx 1000\,\mathrm{C}$, using the anode dimensions given in Fig. 5, it can be finally estimated for $\dot{m} = 5\,\mathrm{mg/s}$ that: (1) – the neutral density inside the holes is $n_H = \dot{m}/(M_n \cdot A_H \cdot \sqrt{T_A / M_n}) = 2.7 \cdot 10^{16}\,\mathrm{cm}^{-3}$, (2) – the static pressure in the holes is $P_H = n_H T_a \approx 3\,\mathrm{Torr}$, and it is twice as big as the dynamic pressure, (3) – the static pressure inside the anode is $P_A = 3/2\, P_H \approx 4.5\,\mathrm{Torr}$, and (4) – the neutral density inside the anode is $n_A \approx 4 \cdot 10^{16}\,\mathrm{cm}^{-3}$. For the neutral-neutral collision cross-section $\sigma_{nn} \approx 3 \cdot 10^{-15}\,\mathrm{cm}^2$, the length of the mean free path inside the holes can be estimated as $\Lambda_H = 1/(\sigma_{nn} \cdot n_H) \approx 0.12\,\mathrm{mm}$, which is smaller than the hole diameter, D_H = 0.3 mm. This estimation supports the aforementioned assumption of the hydrodynamic flow inside the holes. Assume now that after the jets that are coming out of the gas-injecting holes hit the baffles (Fig. 8), the neutral gas spreads out and homogeneously fills up the volume under the baffles. Then, assuming that the neutral gas leaves the volume under the baffles and enters the channel with the velocity of a free atomic flow, $V_a = \sqrt{T_A/(2 \cdot \pi \cdot M_n)} \approx 113\,\mathrm{m/s}$, the average neutral density, neutral pressure, and the length of the mean free path for neutral-neutral collisions under the baffles can be estimated as $n_B \approx \dot{m}/(M_n \cdot V_a \cdot A_B) \approx 5.5 \cdot 10^{14}\,\mathrm{cm}^{-3}$, $P_B = n_B T_A \approx 75\,\mathrm{mTorr}$, and $\Lambda_B = 1/(\sigma_{nn} \cdot n_B) \approx 6\,\mathrm{mm}$, respectively. In the above estimation, $A_B = \pi \cdot (D_{out} + D_{in}) \cdot \Delta_B \approx 3.7\,\mathrm{cm}^2$ is the area of the surface through which the gas leaves the volume under the baffles, calculated using the dimensions given in Fig. 8. Finally, when the neutral gas distributes uniformly[33] over the entire channel cross-section and bleeds through the channel with the velocity V_a, the density, pressure, and the length

of the mean free path near the anode can be estimated as $n_C \approx \dot{m}/(M_n \cdot V_a \cdot A_{coll}) \approx 2.6 \cdot 10^{13}\,\mathrm{cm}^{-3}$, $P_C = n_C T_A \approx 3.5\,\mathrm{mTorr}$, and $\Lambda_C = 1/(\sigma_{nn} \cdot n_C) \approx 12\,\mathrm{cm}$, respectively.

B. Formation of a Negative Fall at the Clean Anode

In the quasineutral plasma between the clean anode and the acceleration region, the electron drift velocity, $V_{dr} \sim I_d/(e \cdot n \cdot A_{coll}) \approx 10^7$ cm/s, is much smaller than the average velocity of the half-Maxwellian electron flux that would be traveling toward the anode in the absence of an electron-repelling anode sheath, $V_{HM} = \sqrt{2T_e/(\pi\, m_e)} \approx 8 \cdot 10^7$ cm/s. The above estimations were made using the channel cross-section equal to $A_{coll} = 77\,\mathrm{cm}^2$, the measured discharged current, $I_d = 4.35\,\mathrm{A}$, and the plasma density, n, along with the electron temperature, T_e, measured in the mid-point between the channel walls at 2 mm from the anode for $V_d = 200$ V and $\dot{m} = 5\,\mathrm{mg/s}$ [Figs. 5 (a) and 6 (a)]. Thus, the thermal electron flux to the anode would carry an electric current much greater than the discharge current. At mass flow rates typical for the 2 kW Hall thruster, electron-neutral collisions are very weak near the anode ($\Lambda_{en} \sim \Lambda_{nn} \approx 12\,\mathrm{cm}$), so is the magnetic field in the conventional configuration.[28] Therefore, formation of an electron-repelling anode sheath (negative anode fall) is required to repel an excessive electron flux from the anode. A reversed electron flux created in the electron-repelling anode sheath decreases the net electron velocity in the quasineutral plasma near the anode to the value V_{dr} determined by the discharge current, thus providing current continuity everywhere.

C. Formation of a Positive Fall at the Coated Anode

In the case of the coated anode (Fig. 8), the electron drift velocity estimated the same way as above, is even smaller, $V_{dr} \approx 5 \cdot 10^6$ cm/s, because for the same operating conditions the plasma density measured near the coated anode is almost twice as big as it is near the clean anode (Fig. 6). Since the electron thermal velocity is almost the same (Fig. 5), formation of an *electron-repelling sheath* at the *coated anode surface* is again required to decrease the net electron velocity in the quasineutral plasma near the anode from V_{HM} to V_{dr}. By reflecting electrons and creating an ion backflow this sheath also allows satisfying the condition of a zero net current to dielectric.

1. Electron-Attracting Anode Sheath

While the anode surface exposed to plasma gets coated with dielectric, some elements of the anode surface, for example the inner side of the gas-mixing baffles or the interior of the gas-injecting holes, may remain conductive (Fig. 8). When the anode front surface is coated with dielectric, the discharge current supposedly closes to the anode at these conductive surfaces by the electrons that are not repelled. A half-Maxwellian electron flux entering the volume under the baffles (Fig. 5) carries the electric current $I_{HM} = 1/2 \cdot (1.5 \cdot n) \cdot \sqrt{2T_e/(\pi m_e)} \cdot e \cdot A_B \approx 1.76\,\text{A}$, which constitutes about 40% of the measured discharge current, $I_d = 4.32\,\text{A}$. The above estimation was made using the plasma density, n, and electron temperature, T_e, measured in the mid-point between the channel walls at 2 mm from the anode for V_d = 200 V and $\dot{m} = 5\,\text{mg/s}$ [Figs. 5 (b) and 6 (b)], and considering the maximum (~50%) relative error in determining the plasma density from biased probe measurements[29]. The remainder 60% of the electron flux supposedly gets drawn in under the baffles by the *electron-attracting sheath* that appears

at the inner, *metal sides of the baffles*. Due to this sheath, the near-anode plasma potential appears to be about 4 – 6 V lower than the anode potential [Fig. 4 (b)]. The plasma in this electron-attracting sheath can be almost purely electron, like in a vacuum diode, since its characteristic scale, $\Delta_B = 0.6\,\text{mm}$ (Fig. 8), is only several Debye lengths estimated at 2 mm from the anode, $\lambda_D = \sqrt{T_e/(4\pi \cdot n_e \cdot e^2)} \sim 0.075\,\text{mm}$. The electron density under the baffles in the case of the coated anode is much larger than in the case of the clean anode, in which only the electrons that penetrate through the electron-repelling sheath enter the volume under the baffles. This could explain such intricate phenomena as distinctive glowing next to each of the gas-injecting holes (where the neutral density is the largest) observed during operation of the 12.3 cm Hall thruster with the coated anode [Fig. 7 (b)].

2. Filamentation

Note that the anode design shown in Fig. 2 is specific to the 12.3 cm Hall thruster in this study; in general, anode may be constructed without gas-mixing baffles[33], or even be separated from a gas distributor[15,34]. Interestingly, operation of a Hall thruster with the coated anode was also observed in the case when the anode design does not include gas-mixing baffles and when there are no gaps between the anode and the channel walls.[35] In this case, the discharge current should close to the anode at the interior of the gas-injecting holes or at the inner side of the anode. To achieve the measured discharge current, the electron density inside the holes should be $n_{eH} \sim I_d/(e \cdot A_H \cdot V_{eH}) \approx 7 \cdot 10^{12}\,\text{cm}^{-3}$, where $V_{eB} \approx 1.3 \cdot 10^8\,\text{cm/s}$ is the velocity of the mono-energetic electron flux accelerated in the potential difference between the anode, $\Phi = 0$, and the plasma, $\Phi = \Phi_{pl} \sim -(4-6)\,\text{V}$, to the energy $E_{eH} = T_e - e\Phi_{pl} \sim 10\,\text{eV}$.

The above estimation is made assuming that Φ_{pl} in the aforementioned work was of the same order as Φ_{pl} in this study. The characteristic voltage drop associated with such electron density, $\Delta\Phi \sim e \cdot n_{eH} \cdot D_H^2 \approx 1.2\,\mathrm{kV}$, is much larger than the plasma potential measured relative to the anode. Therefore, plasma needs to be quasineutral inside the holes, with anode fall supposedly concentrated at the walls of the holes or at the inner anode surface. The mechanism that could be responsible for formation of such ultra high-density plasma channels in front of each hole is not yet understood.

3. Enhanced Ionization

It was observed experimentally for Hall thrusters that penetration of the electrons into the anode cavity can cause ionization of the neutral gas inside the anode.[12] Furthermore, near the anode, the discharge of a Hall thruster with a coated anode can be compared to that of a relatively well-studied hollow-anode plasma source[3,4], as the coated anode has two essential features of the hollow anode: a collecting surface area that is significantly smaller than the cross-sectional area of the discharge chamber, and an insulated front surface. A high degree of ionization inside the hollow-anode plasma source – near-anode electron density of 10^{10} – 10^{11} cm^{-3} at nitrogen flow rate of 25 scc/min – was attributed to formation of a thick electron-attracting anode sheath, in which electrons gain kinetic energy of up to 40 eV.[5] Thus, it can be suggested that formation of a positive fall at the coated anode in the 2 kW Hall thruster could be explained by the need for enhanced ionization: additional ionization in the sheath or inside the anode would increase the electron flux toward anode conductive surfaces to the value determined by the discharge current.[27] However, the neutral gas pressure in front of the anode in a hollow-anode plasma source is about 100 times larger (and therefore the

ionization length is about 100 times smaller) than it is near the coated anode in a Hall thruster.[5] Furthermore, as it was later reported by Melikov in Ref. 13, noticeable ionization inside the anode occurs only if the anode temperature is lower than ~500 C. At higher temperatures, the neutral pressure, $p_n \geq 2\,\text{Torr}$, becomes comparable to the electron pressure, $p_e \sim 1.9\,\text{Torr}$, and the discharge is carried by the gas flow out of the anode cavity (these estimations were made for the plasma density $n = 10^{10}\,\text{cm}^{-3}$, electron temperature $T_e = 8\,\text{eV}$, and mass flow rate of 2 mg/s).

The following estimations can be used to demonstrate that formation of a positive anode fall at the coated anode in the 2 kW Hall thruster is unlikely to be explained by the need for enhanced ionization. For a half-Maxwellian electron flux with the temperature $T_{eB} \sim 10\,\text{eV}$ and neutral densities calculated above, ionization lengths in front of the anode, under the baffles, inside the gas-injecting holes, and inside the anode can be estimated as $\Lambda^i_C \sim 1/(<\sigma^i>\cdot n_C) \approx 1\text{m}$, $\Lambda^i_B \sim 4.5\text{cm}$, $\Lambda^i_H \sim 1\text{mm}$, and $\Lambda^i_A \sim 0.6\text{mm}$, respectively. Here, $<\sigma^i> = <\sigma^i \cdot V_e> / V_{HM} \approx 4\cdot 10^{-16}\,\text{cm}^2$ is the energy-dependent electron impact ionization cross-section for Xenon atoms, averaged over the half-Maxwellian distribution.[28,36] Thus, significant multiplication of the electron flux entering the volume under the baffles could occur only inside the holes or inside the anode. While electrons produced by ionization would reach the metal surface and contribute to the discharge current, corresponding ions would have to stream out into the channel and recombine with electrons at the anode dielectric surface, to provide charge conservation and current continuity everywhere. As follows from the estimations above, the ion flux from the volume under the baffles would then represent about 60% of the discharge

current, so ion density under the baffles can be estimated as $n_{iB} \sim 0.6 \cdot I_d / (e \cdot V_{iB} \cdot A_B) \approx 3.3 \cdot 10^{13} \mathrm{cm}^{-3}$, assuming ions are accelerated in the positive anode fall to the velocity $V_{iB} \sim \sqrt{e \cdot \Phi_{pl} / M_{Xe}} \approx 2 \cdot 10^5 \mathrm{cm/s}$. The plasma density inside the holes would have to be even larger, since $A_B / A_H \sim 100$. However, the plasma densities measured inside the Hall thruster anode,[12] in the vicinity of the anode hole in a hollow-anode plasma source,[5] and at 2 mm from the anode in the 12.3 cm Hall thruster (Fig. 6) were observed to be of the order of $10^{10} - 10^{11} \mathrm{cm}^{-3}$. Thus, additional ionization inside the anode and gas-injecting holes is unlikely to be the process that maintains current balance at the anode surface, from which we conclude that formation of a positive fall at the coated anode is unlikely to be explained by the need for enhanced ionization.

V. SUMMARY AND DISCUSSION

Probe measurements showed that the anode sheath in Hall thrusters can be electron-repelling or electron-attracting, depending on the anode collecting surface area, namely, the anode fall changes from positive to negative upon removal of the dielectric coating, which appears on the anode surface during the normal course of Hall thruster operation. The anode sheath formation in Hall thrusters differs essentially from that in the other gas discharge devices, like a glow discharge or a hollow anode, because the Hall thruster utilizes long electron residence times to ionize rather than high neutral pressures. The positive anode fall formation mechanism suggested in this work can be summarized as follows: (1) – when the anode front surface is coated with dielectric, the discharge current closes to the anode at the surfaces that remain conductive, (2) – a total thermal electron current toward the conductive area is significantly smaller than the discharge current,

therefore an additional electron flux needs to be attracted toward the conductive surfaces by the electron-attracting sheath that appears at these surfaces.

Note that understanding the anode sheath structure in the case of a coated anode might be useful for designing a thruster anode. It is yet unclear how oxygen that forms the anode dielectric coating (oxide layer) gets into the discharge chamber, but since the vacuum facility used in the presented experiments is typical for studies of a Hall thruster, it can be suggested that coating formation is a general issue for laboratory Hall thrusters.[37] Moreover, if oxygen enters the thruster channel along with the xenon propellant, this issue could also be expected for thrusters used in actual space applications. Therefore, when designing an anode (which is not necessarily also a gas distributor) for a HT, one has to ensure that some surfaces will remain conductive if the anode front surface gets coated with a dielectric, so that combined conductive surface area is sufficient for passing a discharge current. Furthermore, the electron energy flux toward these surfaces in the case of a coated anode will be much higher than in the case of a clean anode, in which only the electrons that penetrate through the electron-repelling sheath reach the anode; plus, electrons gain additional kinetic energy while moving inside the electron-attracting sheath toward the anode conductive surfaces. At $V_d = 200\,\mathrm{V}$ and $\dot{m} = 5\,\mathrm{mg/s}$, the power per unit area, deposited at the conductive surfaces of the clean and coated anodes can be estimated as $P_{clean} \sim (I_d / A_{coll}) \cdot (2\,T_e / e + |\Delta\varphi_{sh}|) \sim 1\,\mathrm{W/cm^2}$ and $P_{coated} \sim (I_d / A_B) \cdot (2\,T_e / e + |\Delta\varphi_{sh}|) \sim 17$ W/cm^2, respectively (effect of the secondary electron emission was neglected in this calculation, since the characteristic electron energy at the anode, $E \sim 2\,T_e + e\,|\Delta\varphi_{sh}|$, does not exceed 25 eV for both anodes). Thus,

one also has to ensure that conductive surfaces of the coated anode will not overheat during thruster operation.

Finally, note that the anode dielectric coating might have a positive effect on Hall thruster operation. As was reported in Refs 27 and 28, high-amplitude discharge current oscillations in the 1 – 100 kHz wave band, which are inherent to Hall thrusters,[38] are attenuated by up to a factor of two, when the anode of the 12.3 cm Hall thruster is coated with dielectric. Therefore, it may be suggested that significant mitigation of the oscillations with respect to the initial level, observed in several extensive life tests,[39-43] is associated with formation of the anode dielectric coating.[28]

ACKNOWLEDGEMENTS

The authors are very grateful to Artem Smirnov for his help with analyzing the possible mechanisms of anode fall formation, discussed in Sec. IV of this paper. They would also like to thank Dr. Vladimir Semenov and David Staack for fruitful discussions. The EDS analysis of the anode dielectric coating was performed by Stork MMA Testing Laboratories (Newtown, PA). This work was supported by US DOE Contract No. AC02-76CH0-3073 and NJ Commission for Science and Technology.

REFERENCES

1. I. Langmuir and H. M. Mott-Smith, Gen. Elec. Rev. 27, 449, 538, 616, 761, 810. (1924). See also *The Collected Works of Irving Langmuir*, edited by Suits, C. G. and Way, H. E. (Pergamon, New York, 1961), Vol. 4.
2. B. N. Kliarfeld and N. A. Neretina, Sov. Phys. Tech. Phys. **3**, 271 (1958).
3. V. I. Miljevic, Rev. Sci. Instrum. **55**, 931 (1984).
4. V. I. Miljevic, Appl. Optics **23**, 1598 (1984).
5. A. Anders and S. Anders, Plasma Sources Sci. Technol. **4**, 571 (1995) (Printed in the UK).
6. G. Francis, in *Encyclopedia of Physics*, edited by S. Flugge, Handbuch der Physik, Vd. XXII (Springer, Berlin, 1956), pp. 53 – 208.
7. A. von Engel, *Ionized Gases* (Clarendon, Oxford, 1965), § 8.1.
8. V. L. Granovsky, *Electric Current in Gas. Steady Current* (Nauka, Moscow, 1971), § 58 (in Russian).
9. Yu. P. Raizer, *Gas Discharge Physics* (Springer, Berlin, 1997), § 8.10.
10. L. D. Tsendin, *Zh. Tekh. Fiz*. **56**, 278 (1986).
11. A. I. Morozov, Yu. V. Esinchuk, G. N. Tilinin, A. V. Trofimov, Yu. A. Sharov, and G. Ya. Shchepkin, Sov. Phys. Tech. Phys. **17**, 38 (1972).
12. I. V. Melikov, Sov. Phys. Tech. Phys. **19**, 35 (1974).
13. I. V. Melikov, Sov. Phys. Tech. Phys. **22**, 452 (1977).
14. A. M. Bishaev and V. Kim, Sov. Phys. Tech. Phys. **23**, 1055 (1978).

15. G. Guerrini, C. Michaut, M. Dudeck, A. N. Vesselovzorov, and M. Bacal, Proceedings of the 25th International Electric Propulsion Conference, Aug 1997, Cleveland, OH, IEPC Paper 1997-053.

16. Y. Raitses, J. Ashkenazy and M. Guelman, J. Prop. Power **14**, 247 (1998).

17. Y. Raitses, L. A. Dorf, A. A. Litvak, and N. J. Fisch, J. Appl. Phys. **88**, 1263 (2000).

18. N. J. Fisch, Y. Raitses, L. A. Dorf, and A. A. Litvak, J. Appl. Phys. **89**, 2040 (2001).

19. Y. Raitses, M. Keidar, D. Staack, N. J. Fisch, J. Appl. Phys. **92**, 4906 (2002).

20. J. M. Haas and A. D. Gallimore, Phys. Plasmas **8**, 652 (2001).

21. N. B. Meezan, W. A. Hargus, Jr. and M. A. Cappelli, Phys. Rev. E **63**, Art. No. 026410 (2001).

22. N. Z. Warner, J. J. Szabo and M. Martinez-Sanchez, Proceedings of the 28th International Electric Propulsion Conference, March 2003, Toulouse, France, IEPC Paper 2003-082.

23. E. Ahedo, P. Martinez-Cerezo, M. Martinez-Sanchez, Phys. Plasmas **8**, 3058 (2001).

24. A. Fruchtman, N. J. Fisch, and Y. Raitses., Phys. Plasmas **8**, 1048 (2001).

25. M. Keidar, I. Boyd and I. Beilis, Proceedings of the 38th Joint Propulsion Conference and Exhibit, July 2002, Indianapolis, IN, AIAA Paper 2002-4107.

26. L. Dorf, V. Semenov, Y. Raitses, and N. J. Fisch, Proceedings of the 38th Joint Propulsion Conference and Exhibit, July 2002, Indianapolis, Indiana, AIAA Paper 2002-4246.

27. L. Dorf, Y. Raitses, V. Semenov, and N. J. Fisch, Appl. Phys. Let. **84**, 1070 (2004).

28. L. Dorf, *Studies of Anode Sheath Phenomena in Hall Thrusters*. Ph.D. Dissertation. Princeton University, Princeton, NJ 08544, USA (2004).

29. L. Dorf, Y. Raitses, and N. J. Fisch, Rev. Sci. Instrum., **75**, 1255 (2004).

30. L. Dorf, V. Semenov, and Y. Raitses, Appl. Phys. Let. **83**, 2551 (2003).

31. A. I. Bugrova, L. M. Volkova, V. A. Ermolenko, E. A. Kral'kina, A. M. Devyatov, and V. K. Kharchevnikov, High Temp. **19**, 822 (1981).

32. L. D. Landau and E. M. Lifshitz. In *Course of Theoretical Physics, 2nd edition* (Butterworth-Heinemann, Oxford, 1987), *Vol. 6*.

33. V. Vial, A. Lazurenko, C. Laure, and A. Bouchoule. Proceedings of the 28th International Electric Propulsion Conference, March 2003, Toulouse, France, IEPC Paper 2003-0221.

34. A. I. Morozov and V. V. Savelyev. In *Reviews of Plasma Physics*, edited by B. B. Kadomtsev and V. D. Shafranov (Kluwer Academic/Plenum Publishers, New York, 2000), *Vol. 21*, p. 386.

35. Y. Raitses. Unpublished (1996-1998).

36. D. Rapp and P. Englander-Golden, J. Chem. Phys. **43**, 1464 (1965).

37. A. I. Morozov and V. V. Savelyev. In *Reviews of Plasma Physics*, edited by B. B. Kadomtsev and V. D. Shafranov (Kluwer Academic/Plenum Publishers, New York, 2000), *Vol. 21*, pp. 214, 377.

38. E. Y. Choueiri, *Phys. Plasmas* **8**, 1411 (2001).

39. C. E. Garner, J. E. Polk, K. D. Goodfellow, and J. R. Brophy. Proceedings of the 23rd International Electric Propulsion Conference, September 1993, Seattle, WA, IEPC Paper 1993-091.

40. C. E. Garner, J. R. Brophy, J. E. Polk, and L. C. Pless. Proceedings of the 30th Joint Propulsion Conference and Exhibit, June 1994, Indianapolis, IN, AIAA Paper 1994-2856.

41. T. Randolph, G. Fischer, J. Kahn, H. Kaufman, V. Zhurin, K. Kozubsky, and V. Kim. Proceedings of the 30th Joint Propulsion Conference and Exhibit, June 1994, Indianapolis, IN, AIAA Paper 1994-2857.

42. V. Kim, J. Brophy, M. Day, C. Garner, T. Randolph, A. Sorokin. Proceedings of the 31st Joint Propulsion Conference and Exhibit, July 1995, San Diego, CA, AIAA Paper 1995-2669.

43. B. A. Arhipov, A. S. Bober, R. Y. Gnizdor, K. N. Kozubsky, A. I. Korakin, N. A. Maslennikov, S. Y. Pridannikov. Proceedings of the 24th International Electric Propulsion Conference, September 1995, Moscow, Russia, IEPC Paper 1995-039.

CAPTIONS

Fig. 1: Electric potential axial profile in Hall thrusters. The potential jump toward the anode, $\Delta\varphi > 0$, corresponds to the positive anode fall, and the potential drop, $\Delta\varphi < 0$, corresponds to the negative anode fall.

Fig. 2: Anode of the 2 kW Hall thruster (a) – before and (b) – after thruster operation. Accumulated lifetime > 10 hours.

Fig. 3: (a) The 2 kW laboratory Hall thruster with 12.3 cm outer channel wall diameter.
(b) Simulated radial magnetic field axial profile, $B_r(z)$, used in the experiments.
At R = 49 mm – the midpoint between the channel walls.

Fig. 4: Plasma potential radial profiles, $\Phi_{pl}(R)$, measured with the biased probe in the near-anode region of the 12.3 cm Hall thruster with (a) – clean and (b) – coated anodes at several distances from the anode, $Z = 2-12\,\text{mm}$, and several discharge voltages, $V_d = 200-400\,\text{V}$, for mass flow rate $\dot{m} = 5\,\text{mg/s}$. Zero potential is chosen at the anode.

Fig. 5: Electron temperature radial profiles, $T_e(R)$, measured with the biased probe in the near-anode region of the 12.3 cm Hall thruster with (a) – clean and (b) – coated anodes at several distances from the anode, $Z = 2-12\,\text{mm}$, and several discharge voltages, $V_d = 200-400\,\text{V}$, for mass flow rate $\dot{m} = 5\,\text{mg/s}$.

Fig. 6: Plasma density radial profiles, $N(R)$, measured with the biased probe in the near-anode region of the 12.3 cm Hall thruster with (a) – clean and (b) – coated anodes at several distances from the anode, $Z = 2-12\,\text{mm}$, and several discharge voltages, $V_d = 200-400\,\text{V}$, for mass flow rate $\dot{m} = 5\,\text{mg/s}$.

Fig. 7: Photographs of 12.3 cm Hall Thruster operation with (a) – clean and (b) – coated anodes. As can be seen, operation of the 12.3 cm HT with a coated anode is associated with a visual effect: the gas-injecting holes glow brighter than the rest of the anode.

Fig. 8: Possible mechanism of formation of a positive fall at the coated anode.

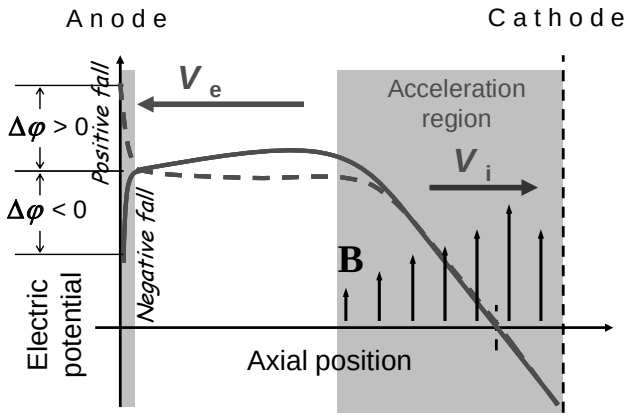

Fig. 1. L. Dorf, Y. Raitses, and N. J. Fisch 2004

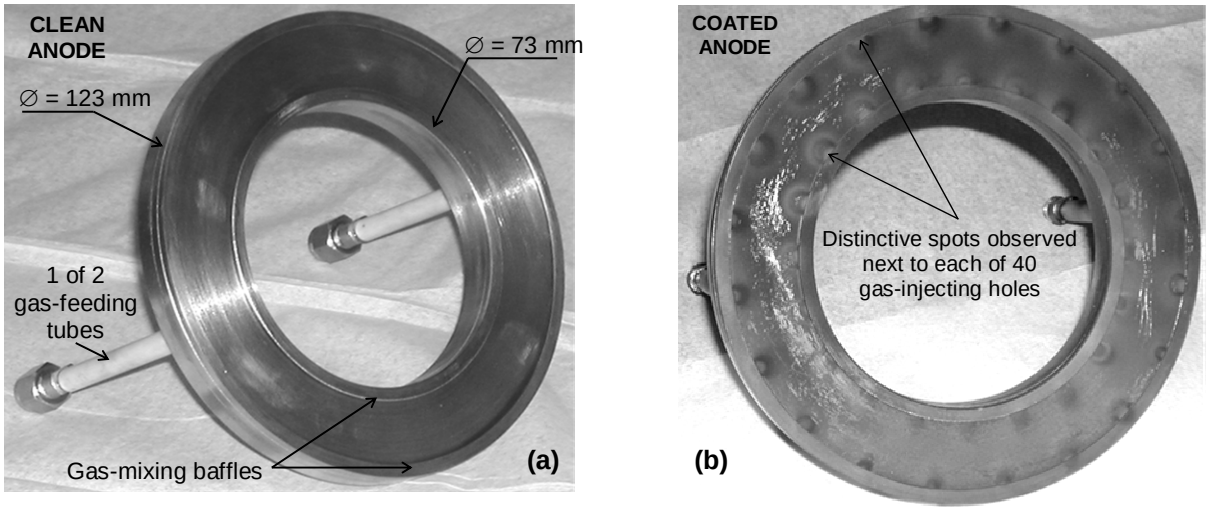

Fig. 2. L. Dorf, Y. Raitses, and N. J. Fisch 2004

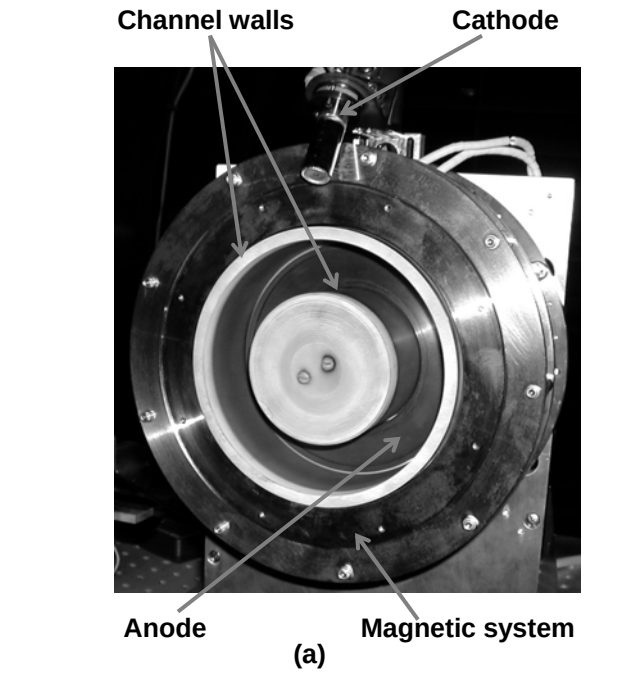

Fig. 3. L. Dorf, Y. Raitses, and N. J. Fisch 2004

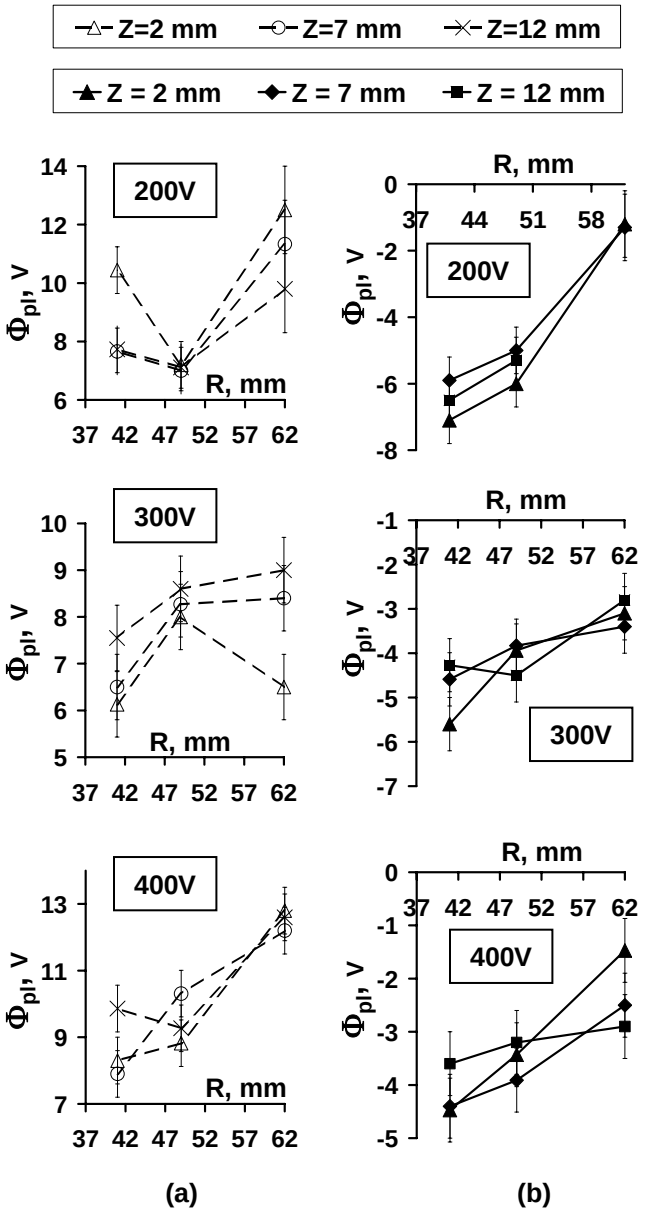

Fig. 4. L. Dorf, Y. Raitses, and N. J. Fisch 2004

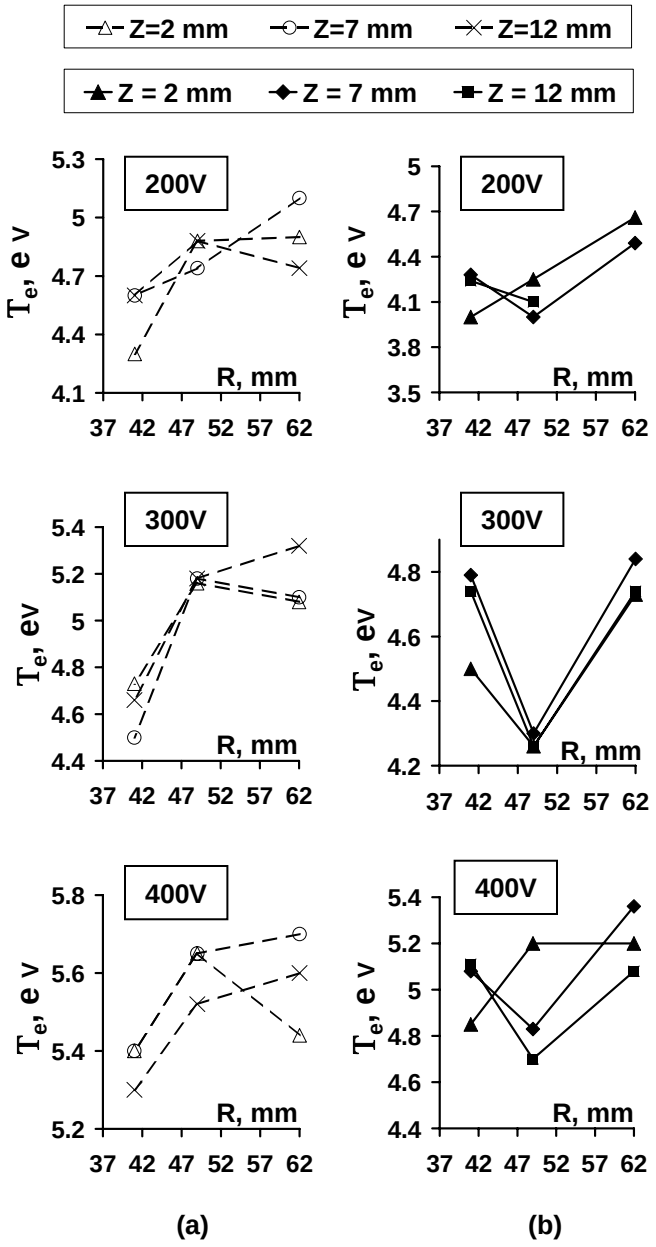

Fig. 5. L. Dorf, Y. Raitses, and N. J. Fisch 2004

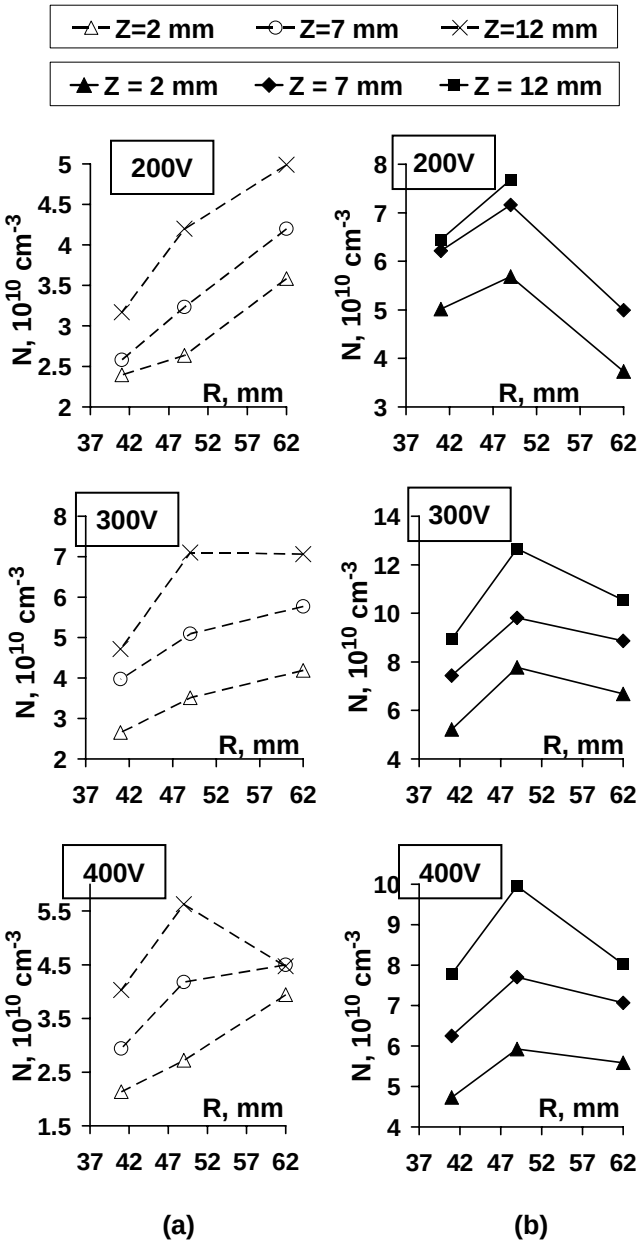

Fig. 6. L. Dorf, Y. Raitses, and N. J. Fisch 2004

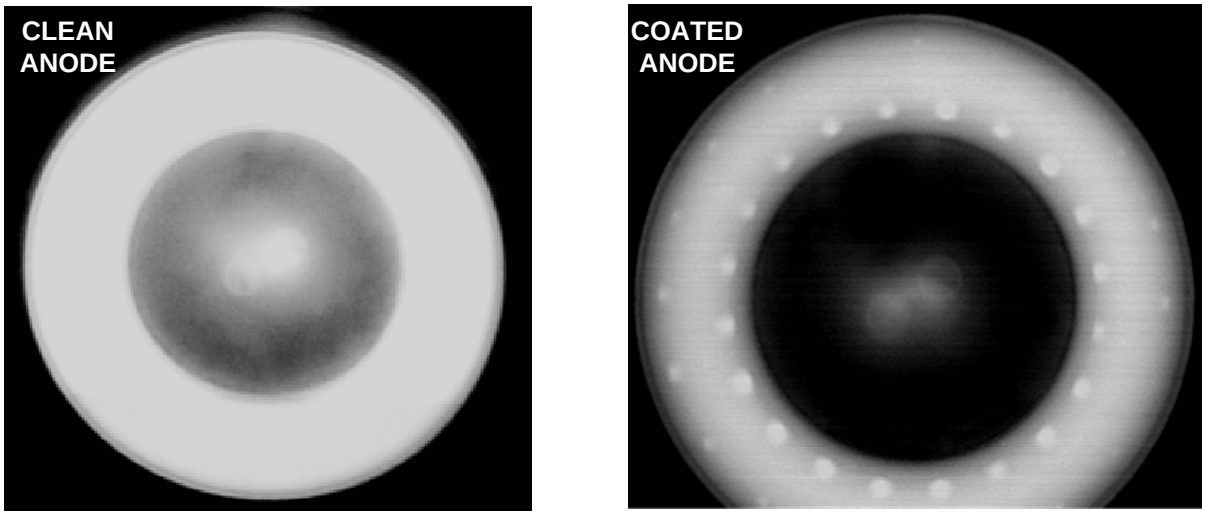

(a) **(b)**

Fig. 7. L. Dorf, Y. Raitses, and N. J. Fisch 2004

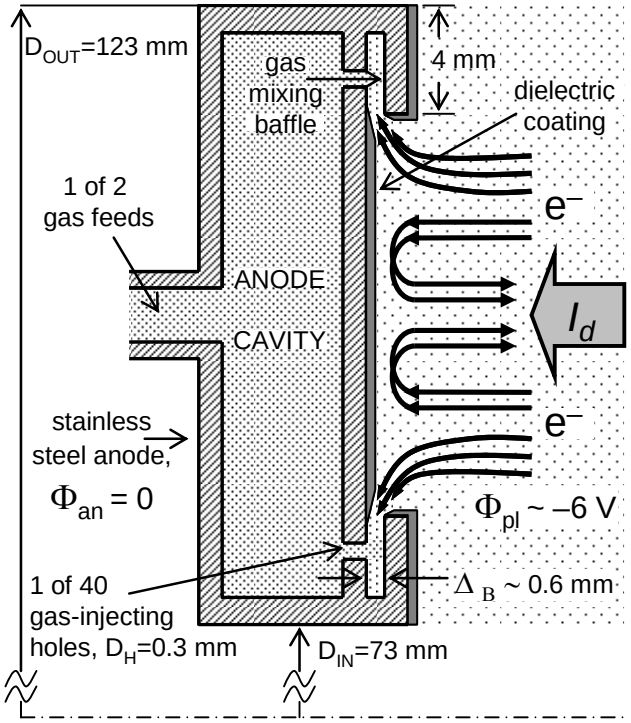

Fig. 8. L. Dorf, Y. Raitses, and N. J. Fisch 2004

External Distribution

Plasma Research Laboratory, Australian National University, Australia

Professor I.R. Jones, Flinders University, Australia

Professor João Canalle, Instituto de Fisica DEQ/IF - UERJ, Brazil

Mr. Gerson O. Ludwig, Instituto Nacional de Pesquisas, Brazil

Dr. P.H. Sakanaka, Instituto Fisica, Brazil

The Librarian, Culham Laboratory, England

Mrs. S.A. Hutchinson, JET Library, England

Professor M.N. Bussac, Ecole Polytechnique, France

Librarian, Max-Planck-Institut für Plasmaphysik, Germany

Jolan Moldvai, Reports Library, Hungarian Academy of Sciences, Central Research Institute for Physics, Hungary

Dr. P. Kaw, Institute for Plasma Research, India

Ms. P.J. Pathak, Librarian, Institute for Plasma Research, India

Ms. Clelia De Palo, Associazione EURATOM-ENEA, Italy

Dr. G. Grosso, Instituto di Fisica del Plasma, Italy

Librarian, Naka Fusion Research Establishment, JAERI, Japan

Library, Laboratory for Complex Energy Processes, Institute for Advanced Study, Kyoto University, Japan

Research Information Center, National Institute for Fusion Science, Japan

Dr. O. Mitarai, Kyushu Tokai University, Japan

Dr. Jiangang Li, Institute of Plasma Physics, Chinese Academy of Sciences, People's Republic of China

Professor Yuping Huo, School of Physical Science and Technology, People's Republic of China

Library, Academia Sinica, Institute of Plasma Physics, People's Republic of China

Librarian, Institute of Physics, Chinese Academy of Sciences, People's Republic of China

Dr. S. Mirnov, TRINITI, Troitsk, Russian Federation, Russia

Dr. V.S. Strelkov, Kurchatov Institute, Russian Federation, Russia

Professor Peter Lukac, Katedra Fyziky Plazmy MFF UK, Mlynska dolina F-2, Komenskeho Univerzita, SK-842 15 Bratislava, Slovakia

Dr. G.S. Lee, Korea Basic Science Institute, South Korea

Institute for Plasma Research, University of Maryland, USA

Librarian, Fusion Energy Division, Oak Ridge National Laboratory, USA

Librarian, Institute of Fusion Studies, University of Texas, USA

Librarian, Magnetic Fusion Program, Lawrence Livermore National Laboratory, USA

Library, General Atomics, USA

Plasma Physics Group, Fusion Energy Research Program, University of California at San Diego, USA

Plasma Physics Library, Columbia University, USA

Alkesh Punjabi, Center for Fusion Research and Training, Hampton University, USA

Dr. W.M. Stacey, Fusion Research Center, Georgia Institute of Technology, USA

Dr. John Willis, U.S. Department of Energy, Office of Fusion Energy Sciences, USA

Mr. Paul H. Wright, Indianapolis, Indiana, USA

The Princeton Plasma Physics Laboratory is operated
by Princeton University under contract
with the U.S. Department of Energy.

Information Services
Princeton Plasma Physics Laboratory
P.O. Box 451
Princeton, NJ 08543

Phone: 609-243-2750
Fax: 609-243-2751
e-mail: pppl_info@pppl.gov
Internet Address: http://www.pppl.gov